This document is a preprint of: A. Trassl, T. Hossler, L. Scheuvens et al., “Deriving an Empirical Channel Model for Wireless Industrial Indoor Communications,” in Proceedings of IEEE 30th Annual International Symposium on Personal, Indoor and Mobile Radio Communications (PIMRC 2019), Istanbul, Turkey, Sep 2019. DOI:10.1109/PIMRC.2019.8904382

Deriving an Empirical Channel Model for Wireless Industrial Indoor Communications

Andreas Traßl[1,2], Tom Hößler[2,3], Lucas Scheuvens[2], Norman Franchi[2], and Gerhard P. Fettweis[1,2,3]
[1]Centre for Tactile Internet with Human-in-the-Loop (CeTI)
[2]Vodafone Chair Mobile Communications Systems, Technische Universität Dresden, Germany
[3]Barkhausen Institut, Dresden, Germany
Email: {andreas.trassl, tom.hoessler, lucas.scheuvens, norman.franchi, gerhard.fettweis}@tu-dresden.de

***Abstract*—Wireless system design on the physical layer is usually evaluated using comprehensive channel models. However, there is still a lack of publicly available stochastic channel models tailored to industrial use cases, which are recently considered more frequently. This paper presents the derivation of such a channel model for the 5 GHz ISM band and its parametrization. The frequency-selective behaviour is modeled by the Saleh-Valenzuela model. Based on a measurement campaign, the parameters of this model for a factory environment are determined and published the first time for the 5 GHz ISM band. Spatial correlation is modeled by the Kronecker model. The temporal variation of the channel is based on a theoretically derived Doppler spectrum assuming Laplacian distributed angle of arrivals. In addition to the description of the model components, key issues and common mistakes while constructing a channel model for industrial applications are discussed in order to advance the design and the deployment of future wireless industrial communications systems. The derived channel model is used in IEEE 802.11ax link layer simulations. It is shown that for industrial use cases specially tailored channel models are needed.**

***Index Terms*—channel model, Saleh-Valenzuela model, power delay profile, industrial environment, WLAN**

I. Introduction

Wireless communications systems have become increasingly common in industrial applications in recent years. The scope of application of wireless systems in this context is diverse and reaches from monitoring to closed-loop control scenarios. Wireless solutions are needed to enable mobile applications, e.g., automated guided vehicles, which allow to flexibly transport factory goods. Another possible use case is the streaming of status information about current machine conditions. Furthermore, wireless systems come along with less maintenance in moving machine parts as established solutions with trailing cable systems and sliding contacts [1]. Thus, wireless communications systems also offer a cost advantage compared to their wired alternative.

Special solutions for the industry, which can deliver ultra reliable low latency communications (URLLC) and could therefore be advantageous for industrial communications for safety-critical and closed-loop control applications, are not available yet. The fifth generation (5G) of mobile communications systems has gathered great interest in this field since transmission latency and dependability are main pillars of the development. Existing approaches for factory automation include, e.g., *WirelessHART* based on IEEE 802.15.4 or the *iWLAN* system built on Wireless Local Area Network (WLAN). Both systems operate in unlicensed frequency bands (ISM bands), which adversely affects the possibility of interference from other users. For WLAN systems, the 5 GHz ISM band is of special interest since compared to the 2.4 GHz band a higher bandwidth is available and less interference can be expected.

The requirements towards transmission latency and dependability in industrial applications are strict and need careful evaluation while developing and deploying a communications system. The dependability highly depends on the physical layer (PHY), which is therefore especially important in the analysis. Wireless system design requires models to simulate effects that occur while transmitting over the channel to design and test the system. Various stochastic channel models are available for different propagation environments and frequency bands. However, the channel conditions in industrial environments are highly characteristic compared to residential or office environments since they are characterized by a great quantity of reflective metal surfaces. Therefore, specially tailored industrial channel models are required in order to develop a suited PHY for industrial use cases. For industrial environments only a few channel models have been developed yet. Extensive studies for ultrawideband (UWB) transmissions have been conducted, proposing channel models with different levels of complexity and different frequency ranges, e.g., [2]. Another popular example is the 802.15.4 channel model, which supports industrial environments and can be used for UWB transmissions within a frequency range from 2 GHz to 10 GHz. A channel impulse response (CIR) model for factory buildings at 1.3 GHz can be found in [3]. Unfortunately, no channel model for industrial environments is proposed for the 5 GHz ISM band yet, which is especially important to WLAN systems.

In this paper, a channel model for industrial indoor environments for transmissions in the 5 GHz ISM band is developed. It combines a path loss (PL) model, log-normally distributed shadowing in regards to large

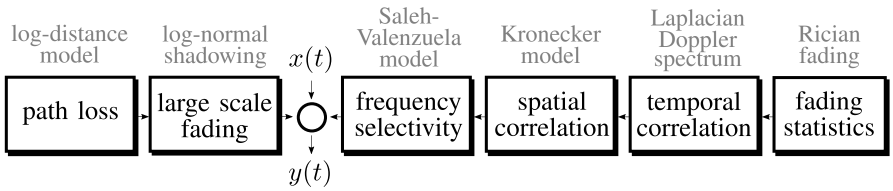

Fig. 1. Overview of the chosen submodel components.

scale fading, and a model for small scale fading. Small scale fading comprises submodel components for temporal correlation, the frequency-selective behaviour of the channel, and spatial correlation to support multiple antenna systems like WLAN systems. These submodel components are conducted in Fig. 1. Furthermore, a measurement-based parametrization for a small factory environment is determined. The described framework allows to extract model parameters for a CIR model from transfer function measurements. A further contribution of this paper is to emphasize key issues and common mistakes while combining model components to an overall channel model and during its parametrization. This paper shows that results obtained using channel models for industrial use cases can differ greatly from currently available models.

II. Path Loss and Large Scale Fading

The decrease of signal power over distance is referred to as PL. Variations in the received signal power over a large distance are modeled as large scale fading usually only considering shadowing. A common PL model also including shadowing is given by

$$\mathrm{PL}(d) = \mathrm{PL}(d_0) + 10n\log\left(\frac{d}{d_0}\right) + X \quad \text{for } d \geq d_0\,, \tag{1}$$

where $\mathrm{PL}(d)$ describes PL and shadowing in dB at distance d. The PL is modeled by means of the reference PL $\mathrm{PL}(d_0)$ measured at distance d_0 and by the PL exponent n. The PL exponent n determines the decrease of power over distance d. The variable X models the influence of shadowing and is on a logarithmic scale additively superimposed to PL. It is well-established to model shadowing by a zero mean log-normal distribution. Its distribution parameter is given by σ_X.

Equation (1) is an empirical model, hence, the model parameters are determined by measurements. For industrial environments and the $5\,\mathrm{GHz}$ ISM band, measurements within factories were carried out and the model parameters were estimated in [4]. The authors distinguish between three topologies: line of sight (LOS) connections, obstructed line of sight (OLOS) connections with industrial inventory on receiver height of $2\,\mathrm{m}$ as well as on transmitter height of $6\,\mathrm{m}$ are considered. The authors tested different model variants, preferring the variant without assumption of free space propagation to the reference distance $d_0 = 15\,\mathrm{m}$. The estimated parameters therefore are reproduced in Tab. I.

III. Small Scale Fading

Rapid changes of the received signal power on a small time scale are described under the term *small scale fading*. This includes effects of multipath propagation and also Doppler frequency shifts induced by movement. The statistics of small scale fading in industrial environments can be modeled as Rician fading [4]. In [4], values of the Rician K-factor were estimated for different factory environments. The values postulated by the authors for an estimator using the least squares (LS) method are summarized in Tab. I.

A. Frequency Selectivity

A communications channel is frequency-selective if signal copies with different propagation delays overlay, e.g., as a result of multipath propagation with different path lengths. All multipath components (MPCs) arriving at the same time at the receiver are denoted as a tap. The system-theoretical description of the mobile radio channel as a linear, time-variant (LTV) and causal system can be used for modeling. When only considering small scale fading this is represented by

$$y(t) = h(t,\tau) * x(t) = \int_0^\infty x(t-\tau)h(t,\tau)d\tau\,, \tag{2}$$

where $y(t)$ is the receive signal and $x(t-\tau)$ is the transmit signal $x(t)$ delayed by the propagation delay τ. The factor $h(t,\tau)$ represents the time-variant impulse response of the radio channel, where $h(t,\tau)$ can be interpreted as an infinite sum of all taps. To allow the implementation, $h(t,\tau)$ has to be restricted to a finite number of taps U. Then, $h(t,\tau)$ is given by

$$\begin{aligned} h(t,\tau) &= \sum_{i=0}^{U-1} h(t,\tau_i)\delta(\tau-\tau_i)\,, \\ &= \sum_{i=0}^{U-1} \beta_i c_i(t)\delta(\tau-\tau_i)\,, \end{aligned} \tag{3}$$

where the i-th tap is characterized by the propagation delay τ_i and the amplitude and phase shift of the tap $h(t,\tau_i)$. The complex value $h(t,\tau_i)$ can further be divided into a complex factor $c_i(t)$ of the time-dependent stochastic fading process – in this paper modeled as Rician fading – and the mean path amplitude β_i as shown in (3).

A widely accepted model for τ_i and β_i for indoor communications is the Saleh-Valenzuela (SV) model, proposed in [5]. The authors assume that MPCs arrive

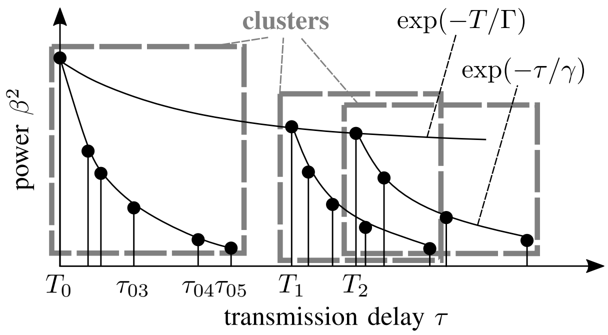

Fig. 2. Overview of the SV model assumptions.

in groups, so called clusters. The arrival time of the l-th cluster is denoted as T_l, while the arrival time of the k-th tap within the l-th cluster is denoted as τ_{kl}. Hence, the relationship to the propagation delay τ_i of the i-th tap is given by

$$\tau_i = T_l + \tau_{kl} \, . \tag{4}$$

They further propose that the arrivals of clusters and also taps within each cluster are modeled as a Poisson process with exponentially distributed interarrival times. The distribution parameters are the cluster arrival rate Λ and the tap arrival rate λ, respectively. In short, the authors state that the arrival times of MPCs can be expressed by

$$\begin{aligned} p(T_l|T_{l-1}) &= \Lambda \exp(-\Lambda(T_l - T_{l-1})) \quad \text{for } l > 0 \, , \\ p(\tau_{kl}|\tau_{(k-1)l}) &= \lambda \exp(-\Lambda(\tau_{kl} - \tau_{(k-1)l})) \quad \text{for } k > 0 \, . \end{aligned} \tag{5}$$

To model the power of the cluster arrivals and the power of taps within each cluster the authors propose exponential power decays. The exponential decay is characterized by the cluster power-decay time constant Γ and the tap power-decay time constant γ, yielding

$$\beta_i^2 = \beta_0^2 \exp\left(-T_l/\Gamma\right) \exp\left(-\tau_{kl}/\gamma\right) . \tag{6}$$

A schematic summary of the model assumptions is given in Fig. 2. Values for the SV model parameters Λ, λ, Γ and γ for different environments and frequency ranges can be found in the original model publication [5] and were re-estimated in many other publications. For industrial communications, parameter estimation was carried out mainly for UWB transmissions at various frequency ranges. However, for the $5\,\mathrm{GHz}$ ISM band, no parameter estimation is published yet to the best of our knowledge. However, measurement data, which can be used for the parametrization, is publicly available, e.g., the measurement campaign in [6]. Therein, the channel gain was measured discretely over time and frequency in a small hall with an extension of roundly $10\,\mathrm{m} \times 30\,\mathrm{m}$ containing industrial inventory. The measurement was carried out at $5.8\,\mathrm{GHz}$ center frequency with a span of $1\,\mathrm{GHz}$, which is close to the $5\,\mathrm{GHz}$ ISM band. The duration of one measurement was $17\,\mathrm{s}$ during which a person was moving once back and forth in front of the receiving antenna. Apart from this, the environment was static. At any time the authors observed an OLOS connection. They measured at three different transmission distances $3.1\,\mathrm{m}$, $10\,\mathrm{m}$, and $20.4\,\mathrm{m}$.

The SV model parameters can be estimated under use of the power delay profile (PDP), which characterizes the connection between transmission delay and channel gain. To obtain the PDP from a measurement of channel gain over frequency, a conversion under use of the Bello functions can be done: The input delay spread function, which is the square root of the PDP, can be determined by calculating the inverse Fourier transform with respect to frequency of the time-variant transfer function. Since only discrete data is available, the inverse discrete Fourier transform (IDFT) has to be used to calculate a sampled version of the input delay spread function. In this discrete version, the exact position of a MPC is not directly visible. Therefore, MPCs have to be identified in an additional step.

The identification of MPCs is difficult since the discrete time-variant transfer function only consists of a finite number of samples. This equals rectangular windowing in time domain, also affecting the input delay spread function as the different MPCs are convoluted with a sinc-function. The challenge is that the main lobe of the sinc-function belongs to a MPC which must be identified, while the different side lobes shall not be identified as MPCs. Furthermore, the side lobes cause amplitude errors in adjacent MPCs. Instead of rectangular windowing alternative windowing functions can be used. The windowing function has to be chosen carefully as a trade-off between the width and steepness of the main lobe, which could conceal neighboring MPCs and the size of the side lobes, which cause amplitude errors and may be falsely detected as MPCs. For the measurement series in [6], a Hamming window is well-suited since it has the smallest first side lobe next to the main lobe of all windowing functions. As the MPCs in [6] are close together, this results in the lowest number of concealed MPCs and also leads to less falsely detected MPCs near the main lobe. In return, the side lobes of the windowing function are decreasing more slowly compared to other available windowing functions and the main lobe is twice as wide as the main lobe of a rectangular window.

Additionally to the influence of the windowing function, the exact position of the main lobes center is not known due to the discrete nature of the samples in the input delay spread function. The application of zero padding before calculating the IDFT determines the main lobes' centers more accurate. Each local maximum can – after application of zero padding – be identified as a MPC. The proposed signal processing is exemplarily illustrated in Fig. 3. The complete determined PDP for a

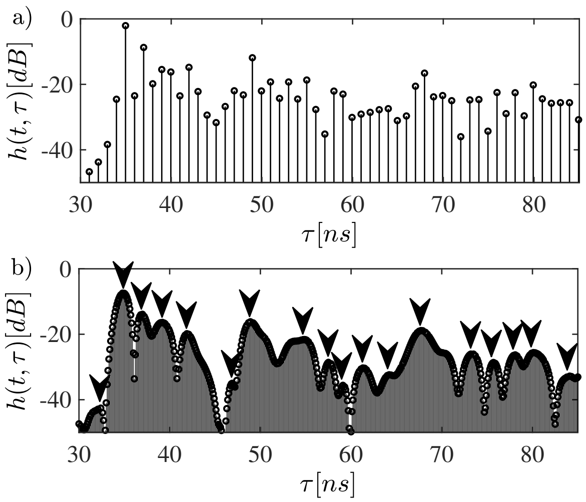

Fig. 3. Cutout of the impulse response at $t = 0$, determined from the measurement series in [6] using a) rectangular windowing and b) a Hamming window and zero padding, the maxima are marked by arrows and identified as MPCs.

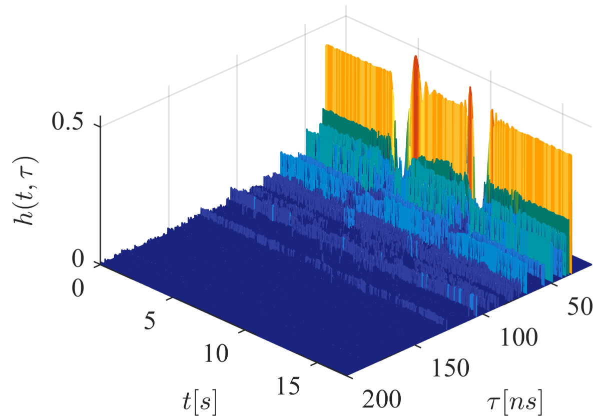

Fig. 4. Time-variant impulse response, determined from the measurement series in [6] with $20.4\,\mathrm{m}$ transmitter receiver distance.

transmitter-receiver-distance of $20.4\,\mathrm{m}$ is shown in Fig. 4. The movement of a person in front of the antenna is clearly visible. The two collapses of the first tap occur when the person was within the direct path between the antennas. All identified MPCs below the noise floor are discarded for further processing.

After squaring the input delay spread function to obtain the PDP, the SV model parameters are determined in two steps: Firstly, each tap has to be associated with a cluster, the process of which is known as clustering. After that, the parameters can be estimated. Clustering is often done by visual inspection, for example in [7]. Obviously, this procedure is highly subjective and therefore results in different model parameters depending on the inspector's assessment. Unfortunately, no ideal algorithmic approach is available yet, either. In [8], a clustering algorithm based on intuitive assumptions is published. The authors propose to test different numbers of clusters. For each possible association of taps to clusters the error of a linear regression in semi-logarithmic scale over the taps of one cluster is calculated. The algorithm terminates when a user-defined regression-error is reached. As a result of the small number of input parameters, this algorithm can support the process of visual inspection. However, since it is based on a user defined termination, it will also provide subjective results. For the measurement series in [6], a mean quadratic error of $2\,\mathrm{dBm}$ was chosen after several test runs following the procedure described in [8]. Since all taps are close to each other, no cluster can be observed only as a reason of a great time separation between two taps. This additional criterion for clustering defined in [8] is therefore not used here.

After clustering, the model parameters Λ and λ are estimated using the minimum variance unbiased estimators given by

$$\hat{\Lambda} = \frac{N_{\Delta T}}{\sum_{l=1}^{N_{\Delta T}}(\Delta T)}, \quad \hat{\lambda} = \frac{N_{\Delta\tau}}{\sum_{k=1}^{N_{\Delta\tau}}(\Delta\tau)}, \tag{7}$$

where $\hat{\Lambda}$ is the estimated value of the cluster arrival rate Λ, calculated from $N_{\Delta T}$ observed cluster inter-arrival times ΔT taken from all measured transmission distances and time instances. The variable $\hat{\lambda}$ denotes the estimated value for λ, calculated by means of $N_{\Delta\tau}$ observed tap inter-arrival times $\Delta\tau$. Only similar PDPs are used for parameter estimation. This means PDPs with collapses in the first tap due to the movement of a person in front of the antenna are excluded.

The estimation of the values $\hat{\Gamma}$ and $\hat{\gamma}$ can be conducted by LS fitting of an exponential function to the data. Please note that a linear LS fit of the data in logarithmic scale is not optimal in the LS-sense and will lead to different model parameters. The fit for $\hat{\Gamma}$ is done by shifting all cluster arrivals of each measurement series untill the first arrival is at $\tau = 0\,\mathrm{ns}$. Furthermore, all arrivals are scaled such that the first arrival has a power of $0\,\mathrm{dBm}$. By doing so, it has to be noted that the noise is also scaled. Therefore, weighting according to the power of the first cluster arrival is considered in the LS fit. The fit to obtain $\hat{\gamma}$ is performed analogously.

All estimated parameter values are presented in Tab. I. The smaller value of Λ compared to the original model parameter postulated in [5] is most likely due to the smaller hall size. Furthermore, we assume that the higher carrier frequency is mainly responsible for the smaller values of Γ and γ. To allow the implementation a modeling threshold has to be defined since only a finite number of taps can be simulated. With a threshold of $-25\,\mathrm{dBm}$, which is also used for the WLAN models, and the postulated parameters a mean root mean square delay spread (RMSDS) of $7.6\,\mathrm{ns}$ is achieved. The RMSDS is related to the coherence bandwidth and therefore offers a measure how fast the channel changes over frequency. This value is quite small compared to other channel models which seem to be suitable for industrial environments, e.g., the WLAN channel model E. The WLAN channel model E has a RMSDS of $100\,\mathrm{ns}$. The small RMSDS of the proposed model is most likely due to the small dimensions of the room. Therefore, we recommend to apply the estimated parameters to model small factory halls only.

B. Spatial Correlation

Many models are available characterizing the spatial correlation between the transmission paths of a multi-antenna system. Commonly used is the Kronecker model, e.g., in the WLAN channel models. For more complex models, as the Weichselberger model for example, no parameters for industrial environments are publicly available yet. The Kronecker model is parametrized only by the power azimuth spectrum (PAS) on transmitter and receiver side, analyzed in multiple publications and also has suitable parameters available. Therefore it is used in this paper. The function $\mathrm{PAS}(\Theta)$ describes the relationship between transmitted or received signal power depending on whether the correlation is calculated at the transmitter or the receiver and the azimuth angle. This model should only be used to predict the spatial correlation for a maximum of two transmit and two receive antennas [9]. For a higher number of antennas, applying more complex models is recommended.

In [10] it was found that for indoor environments the mean angle of arrival (AoA) of different clusters are uniformly distributed. According to the authors, the AoAs of taps within a cluster are Laplacian distributed with the angular spread (AS) σ as distribution parameter. For a system like WLAN, it can be assumed that these findings are also valid for the angle of departure, since the WLAN access point is in a similar environment as the WLAN station. Thus, a Laplacian-distributed PAS on transmit and receiver side is applied in the following. Since measurements for the AS for industrial environments to parametrize the Laplacian PAS are not publicly available yet, measurements in different indoor environments are used. For a center frequency of $5.2\,\mathrm{GHz}$ the AoA was $\sigma = 16.69°$ and $\sigma = 41.25°$ in two office buildings [11]. The measurements were carried out for the same center frequency in [12] in a big indoor environment, an office, and an electrical laboratory. The authors could investigate an AS between $\sigma = 3.93°$ and $\sigma = 9.03°$. Since high differences between the different measurements can be observed, we conclude that the AS is highly dependent on the environment and other external factors. Regarding the channel model in this work two extreme values for the AS are selected, see Tab. I.

C. Temporal Correlation

The variation of the channel over time is determined by the Doppler power density spectrum Φ_{cc}. Measurements of the Doppler power density spectrum in industrial environments are available, e.g., in [13], but no functional description of the spectrum is presented. Other published measurements in industrial environments are not available to the best of our knowledge. The WLAN channel models, which are commonly used for WLAN systems, use a bell shaped Doppler spectrum. This Doppler spectrum shall mimic a static transmitter and receiver with movement in the environment. However, the circumstances of the measurement or underlying assumptions that lead to the bell shaped Doppler spectrum are not documented. Alternatively to measurement based Doppler spectra, theoretical derived spectra can be used. The most common theoretical derived Doppler spectrum is the bathtub-shaped Jake’s spectrum. This spectrum is based on the assumption of equally distributed AoAs only arriving in the horizontal plane while transmitter or receiver are moving. It is important to note that the assumption for the AoAs if using a theoretical spectrum has to match with previous assumptions. Using the Jake’s spectrum blindly is a common mistake, e.g., observable in [14]. The authors describe the use of the Jake’s spectrum, amongst others. Simultaneously, they propose the use of a Laplace distribution for the AoAs of different taps to model spatial correlation. These are mutually exclusive assumptions. Uniformly distributed AoAs of MPCs of one tap needed to derive the Jake’s spectrum have no mean which therefore cannot be Laplacian distributed. Since MPCs arriving at the same time at the receiver and differently delayed MPCs forming different taps have the same physical cause, it is appropriate to use the same distribution for both phenomena. Hence, we assume a Laplace distribution with the same parameters ϕ and σ as the AoA distribution of the belonging cluster for the AoAs of MPCs of the respective tap, too.

Under these assumptions, the Doppler spectrum for a moving transmitter or receiver with Laplace-distributed AoAs and rays arriving only in the horizontal plane follows as

$$\begin{aligned}\Phi_{\mathrm{cc}}(f_{\mathrm{d}}) = & \frac{\frac{1}{\sqrt{2}\sigma}\exp(-|\frac{\sqrt{2}}{\sigma}(\cos^{-1}(f_{\mathrm{d}}/f_{\mathrm{m}})-\phi)|)}{|f_{\mathrm{m}}\sqrt{1-(f_{\mathrm{d}}/f_{\mathrm{m}})^2}|} \\ & + \frac{\frac{1}{\sqrt{2}\sigma}\exp(-|\frac{\sqrt{2}}{\sigma}(\cos^{-1}(f_{\mathrm{d}}/f_{\mathrm{m}})+\phi)|)}{|f_{\mathrm{m}}\sqrt{1-(f_{\mathrm{d}}/f_{\mathrm{m}})^2}|} \\ & \text{for } |f_{\mathrm{d}}| \leq f_{\mathrm{m}}\,. \end{aligned} \quad (8)$$

Otherwise, for $|f_{\mathrm{d}}| > f_{\mathrm{m}}$, it holds that $\Phi_{\mathrm{cc}} = 0$. The Doppler frequency is denoted by f_{d} with the maximum Doppler frequency f_{m}. The maximum Doppler frequency f_{m} is defined by the relative movement speed between transmitter and receiver v, the speed of light c and the carrier frequency f_{c} according to $f_{\mathrm{m}} = \frac{v}{c} f_{\mathrm{c}}$. The Doppler spectrum (8) is visualized in Fig. 5 for different parameters of the AS σ. For very high values of σ the used Doppler spectrum approaches the Jake’s spectrum.

The Doppler spectrum is completely defined by the

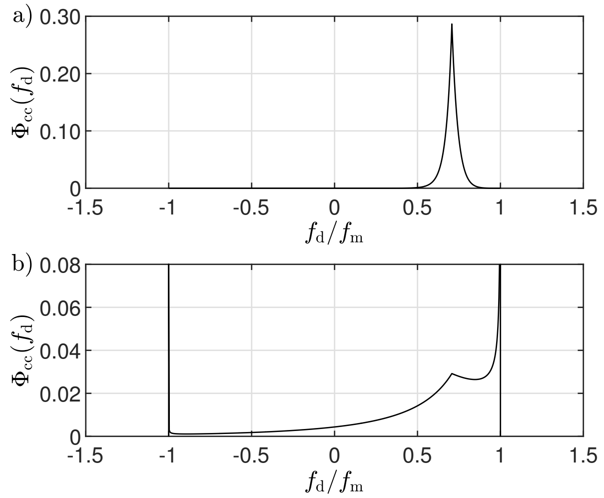

Fig. 5. Doppler spectrum with Laplacian AoA and rays arriving only in the horizontal plane for $\phi = \frac{\pi}{4}$, $f_{\mathrm{m}} = 50\,\mathrm{Hz}$ and different values for the AS a) $\sigma = 4°$ and b) $\sigma = 41°$.

carrier frequency f_{c} and the relative movement speed v. Assuming a static access point, only the movement speed of the station has influence. We focus on the following exemplary settings: in industrial applications, a transceiver could be attached on the head of a robotic arm to replace cables. A, fully extended robotic arm can move at a speed of $360\,°/\mathrm{s}$ at a maximum radius of $0.7068\,\mathrm{m}$ as stated in its data sheet. Such a robotic arm achieves a maximum movement speed of roundly $4.4\,\mathrm{m/s}$. Another class of moving machinery in factories are automated guided vehicles, which are moving at about $1\,\mathrm{m/s}$. These values are summarized in Tab. I.

If transmitter and receiver are static but scatterers in the environment move, differently shaped Doppler spectra are obtained. In these cases Doppler spectra with a peak around $f_{\mathrm{d}}/f_{\mathrm{m}} = 0$ can be observed [15].

TABLE I
PARAMETERS OF THE CHOSEN MODEL COMPONENTS FOR AN INDUSTRIAL INDOOR CHANNEL IN THE 5 GHz ISM BAND.

model	scenario	parameters
pathloss and shadowing	LOS	$\mathrm{PL}(d_0) = 77.57\,\mathrm{dB}$, $n = 1.25$, $\sigma_x = 4.32\,\mathrm{dB}$
	OLOS, receiver height obstacles	$\mathrm{PL}(d_0) = 81.06\,\mathrm{dB}$, $n = 0.68$, $\sigma_x = 3.87\,\mathrm{dB}$
	OLOS, transmitter height obstacles	$\mathrm{PL}(d_0) = 83.33\,\mathrm{dB}$, $n = 1.35$, $\sigma_x = 3.16\,\mathrm{dB}$
fading distribution	automated production	$K = 16.2\,\mathrm{dB}$
	partially automated production	$K = 14.9\,\mathrm{dB}$
	manual production	$K = 6.5\,\mathrm{dB}$
frequency selectivity	small factory hall	$\Gamma = 11\,\mathrm{ns}$, $\gamma = 1.8\,\mathrm{ns}$, $\Lambda = 17.5\,\mathrm{ns}$, $\lambda = 4.7\,\mathrm{ns}$
spatial correlation	environment with high AS	$\sigma = 41°$
	environment with small AS	$\sigma = 4°$
temporal correlation	robotic arm	$v = 4.4\,\mathrm{m/s}$
	automatic guided vehicle	$v = 1\,\mathrm{m/s}$

IV. RESULTING CHANNEL MODEL

Applying the introduced industrial channel model to analyze the upcoming WLAN standard IEEE 802.11ax, an exemplary packet error rate (PER) simulation is presented in this section. Under the chosen simulation parameters, it is shown that results generated with the proposed industrial channel model greatly differ from available channel models for the 5 GHz ISM band, e.g., the WLAN channel models. Consequently, the importance of deriving adequate channel models for industrial use cases is discussed.

The industrial channel model is simulated for the highest Rician K-Factor in Tab. I of $16.2\,\mathrm{dB}$, as it could be observed that the K-Factor has only a small influence in this type of simulation. All chosen movement speeds and AS parameters are simulated. WLAN channel models are commonly used for simulating indoor environments. The WLAN model variant E is stated to characterize large indoor environments or warehouses and therefore is a suitable WLAN channel model for industrial environments regarding the state of art. Thus, the proposed model is compared with the WLAN channel model variant E. As a communications technology the IEEE 802.11ax standard is used, which is available in *Mathworks' WLAN system toolbox*. Exemplary single user packet transmissions with a PHY payload of $1000\,\mathrm{bytes}$ and $20\,\mathrm{MHz}$ bandwidth with one sending antenna are simulated. The modulation and coding sheme (MCS) is set to MCS0, corresponding to BPSK modulation and code rate 1/2. The shortest guard interval with $0.8\,\mu\mathrm{s}$ duration is used and convolutional channel coding is applied. The longest available channel estimation preamble field is transmitted. On the receiver side, two antennas in combination with maximum ratio combining is used to show the influence of the spatial correlation model. Timing synchronization as well as frequency synchronization is used on receiver side as in real WLAN systems.

The PER results under use of the Monte-Carlo method for these assumptions are presented in Fig. 6. By comparing the two channel models, it is clearly visible

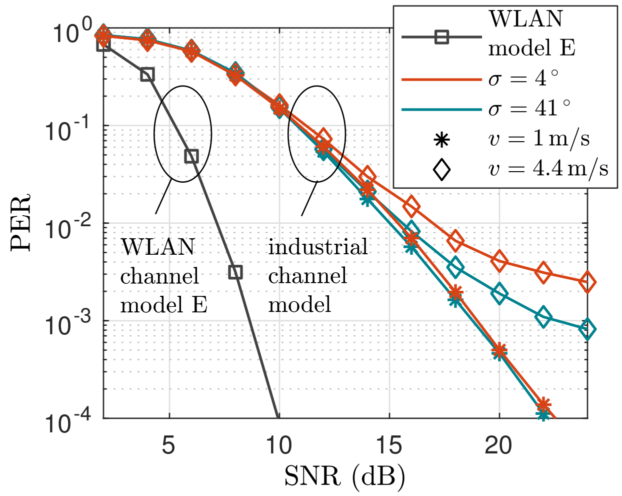

Fig. 6. Simulated PER of IEEE 802.11ax transmissions comparing the proposed industrial channel model for different movements speeds and ASs to the WLAN channel model E.

that the communications system transmitting over the industrial channel model performs worse than over the WLAN channel Model E for all SNR values. The smaller coherence bandwidth of the channel has the highest impact resulting in a smaller channel coding gain. The higher Doppler shift ensures that the channel estimation outdates over the length of a WLAN packet for high movement speeds. It is shown that results generated with the proposed industrial channel model can greatly differ from available channel models, which intuitively may seem adequate for performance simulation of wireless system design intended to serve industrial use cases. Hence, for evaluating wireless industrial applications it is important to carefully select or derive channel models, considering the correct factory size and appropriate movement patterns, in order to avoid misleading results.

V. Conclusion

In this paper, the derivation of a stochastic channel model for transmissions in the 5 GHz ISM band in an industrial indoor environment was presented. We discussed mistakes and inaccuracies in the literature, which should be avoided while creating channel models, e.g, using incompatible model components, subjective methods and non-optimal parameter estimators. A procedure of deriving a channel model for industrial use cases and its parametrization was presented. Additionally, parameter estimation was carried out for a small-sized factory environment providing novel SV model parameters for industrial wireless communications in the 5 GHz ISM band. A *MATLAB* implementation of the proposed channel model will be gladly provided upon request. Based on the shown simulations, we conclude that it is important to utilize tailored channel models for factory environments in order to deliver accurate results, especially with respect to the development of URLLC technologies for industrial applications.

Acknowledgments

This work was in part funded by the German Research Foundation (DFG, Deutsche Forschungsgemeinschaft) as part of Germany’s Excellence Strategy – EXC 2050/1 – Project ID 390696704 – Cluster of Excellence “Centre for Tactile Internet with Human-in-the-Loop” (CeTI) of Technische Universität Dresden. This work was also in part sponsored by the Federal Ministry of Education and Research within the program “Twenty20 – Partnership for Innovation” under contracts 03ZZ0528E – “fast robotics” – and 03ZZ0510F – “fast automation”, respectively.

References

[1] A. Frotzscher, U. Wetzker, M. Bauer, M. Rentschler, M. Beyer, S. Elspass, and H. Klessig, “Requirements and current solutions of wireless communication in industrial automation,” in *2014 IEEE Int. Conf. on Commun. Workshops*, 2014.

[2] A. F. Molisch, D. Cassioli, C. Chong, S. Emami, A. Fort, B. Kannan, J. Karedal, J. Kunisch, H. G. Schantz, K. Siwiak, and M. Z. Win, “A comprehensive standardized model for ultrawideband propagation channels,” *IEEE Trans. Antennas Propag.*, vol. 54, no. 11, 2006.

[3] T. S. Rappaport, S. Y. Seidel, and K. Takamizawa, “Statistical channel impulse response models for factory and open plan building radio communicate system design,” *IEEE Trans. Commun.*, vol. 39, no. 5, 1991.

[4] E. Tanghe, W. Joseph, L. Verloock, L. Martens, H. Capoen, K. V. Herwegen, and W. Vantomme, “The industrial indoor channel: large-scale and temporal fading at 900, 2400, and 5200 MHz,” *IEEE Trans. Wireless Commun.*, vol. 7, no. 7, 2008.

[5] A. A. M. Saleh and R. Valenzuela, “A statistical model for indoor multipath propagation,” *IEEE J. Sel. Areas Commun.*, vol. 5, no. 2, 1987.

[6] D. Block, N. H. Fliedner, and U. Meier, “CRAWDAD dataset init/factory (v. 2016-06-13),” https://crawdad.org/init/factory/20160613/factory1-channel-gain, June 2016.

[7] J. Karedal, S. Wyne, P. Almers, F. Tufvesson, and A. F. Molisch, “Statistical analysis of the uwb channel in an industrial environment,” in *IEEE 60th Veh. Technol. Conf.*, vol. 1, 2004.

[8] J. Chuang, S. Bashir, and D. G. Michelson, “Automated identification of clusters in uwb channel impulse responses,” in *2007 Can. Conf. on Elect. and Comput. Eng.*, 2007.

[9] M. Ozcelik, N. Czink, and E. Bonek, “What makes a good mimo channel model?” in *IEEE 61st Veh. Technol. Conf.*, vol. 1, 2005.

[10] Q. H. Spencer, B. D. Jeffs, M. A. Jensen, and A. L. Swindlehurst, “Modeling the statistical time and angle of arrival characteristics of an indoor multipath channel,” *IEEE J. Sel. Areas Commun.*, vol. 18, no. 3, 2000.

[11] T. Zwick, C. Fischer, and W. Wiesbeck, “A stochastic multipath channel model including path directions for indoor environments,” *IEEE J. Sel. Areas Commun*, vol. 20, no. 6, 2002.

[12] C.-C. Chong, C.-M. Tan, D. I. Laurenson, S. McLaughlin, M. A. Beach, and A. R. Nix, “A new statistical wideband spatio-temporal channel model for 5-GHz band wlan systems,” *IEEE J. Sel. Areas Commun*, vol. 21, no. 2, 2003.

[13] D. Hampicke, A. Richter, A. Schneider, G. Sommerkorn, R. S. Thoma, and U. Trautwein, “Characterization of the directional mobile radio channel in industrial scenarios, based on wideband propagation measurements,” in *IEEE 50th Veh. Technol. Conf.*, vol. 4, Nov. 1999.

[14] E. Kunnari and J. Iinatti, “Stochastic modelling of rice fading channels with temporal, spatial and spectral correlation,” *IET Commun.*, vol. 1, no. 2, 2007.

[15] J. B. Andersen, J. O. Nielsen, G. F. Pedersen, G. Bauch, and G. Dietl, “Doppler spectrum from moving scatterers in a random environment,” *IEEE Trans. Wireless Commun.*, vol. 8, no. 6, 2009.